sciendo

Polish Journal of Chemical Technology, 20, 4, 49—59, 10.2478/pjct-2018-0054

Characterization and optimization of spectrophotometric colour removal from dye containing wastewater by Coagulation-Flocculation

I.A. Obiora-Okafo[1], O.D. Onukwuli[2]

[1]Department of Chemical Engineering, Faculty of Engineering and Technology, Madonna University, Elele, Nigeria
[2]Department of Chemical Engineering, Faculty of Engineering, Nnamdi Azikiwe University, Awka, Nigeria
**Corresponding authors: e-mail: ifyobioraokafo@yahoo.com; onukwuliod@yahoo.com*

The performance of *Vigna unguiculata* coagulant (VUC) for colour removal from acid dye was investigated in this study. The proximate, structure and morphology of the coagulant were investigated using standard official methods, Fourier-Transform Infrared (FTIR) spectrometer and scanning electron microscopy (SEM), respectively. Response surface methodology (RSM) using face-centred central composite design (FCCD) optimized four process variables including pH, coagulant dosage, dye concentration and time. The colour removal efficiency obtained from the optimization analysis was 99.26% at process conditions of pH 2, coagulant dosage 256.09 mg/l, dye concentration 16.7 mg/l and time 540 min. The verification experiments agreed with the predicted values having a standard error value of 1.96%. Overlay contour plot established optimum areas where the predicted response variable is in an acceptable range (≥ 70%) with respect to optimum conditions. The FCCD approach was appropriate for optimizing the process giving higher removal efficiency when compared to the main effect plots.

Keywords: Coagulation-flocculation, natural organic polymer, fibre-metric analysis, spectrophotometer, face-centred central composite design.

INTRODUCTION

There has been an environmental public health problem across the globe in which one major causes is from wastewater discharge. Dyes and pigments are among these contaminants present in wastewater discharge[1]. Presently, about 10,000 commercial dyes and pigments are being used and over 7.11 X 10^7 kg/yr is produced worldwide[2]. Industries that use dye including textile, rubber, pulp, paper, plastic, cosmetics, food, pharmaceutical, leather tanning, printing, and medicine produce dye wastewaters characteristically high in colour, organic and inorganic contents. These dye wastewaters are toxic, carcinogenic, slow down self-purification of streams by reducing light penetration, retard photosynthetic activity and inhibit the growth of biota[3]. Therefore, dye wastewaters generated from industrial applications have to be treated to accord with discharging limit[4].

Dyes are classified as anionic (direct, acid and reactive dyes), cationic (basic dyes) and non-ionic (disperse dyes). Anionic dyes are the largest class of dyes used in the world[5]. In aqueous solution, anionic dyes carry a net negative charge due to the presence of sulphonate (SO_3^-) groups. Acid dyes are anionic compounds characterized by the existence of azo bond (R-N=N-R_2) and mostly belonged to azo and anthraquinone groups. Removal of contaminants from a dye containing wastewaters is often difficult because of their highly soluble and semi-soluble nature[6]. Their complex aromatic structure, synthetic origin, and difficult to be biodegraded also make acid dyes difficult to treat[4]. Biebrich scarlet or acid red 66 (AR 66) is a dark, brownish powdered azo dye. Applications of Biebrich scarlet are useful in fabrics dyeing including wool, silk, polyurethane fibres, and nylon. It is also used as a plasma stain and to impart colour to pharmaceutical preparations[7].

The methods used for contaminant removals from dye wastewater could be divided into three main categories; physical, chemical, and biological. Physical treatments such as nanofiltration[8], membrane filtration[9], ozonation, and adsorption are widely used techniques. Physic-chemical treatment methods are coagulation-flocculation, precipitation, photo-catalysis, oxidation and chemical sludge oxidation. Biological treatment techniques used are aerobic degradation, anaerobic degradation, and living/dead microbial biomass[10]. Coagulation-flocculation has also been integrated with other recent technologies, such as membrane filtration, nanofiltration, to improve the pollutant removal efficiency. Coagulation-flocculation technique has been vastly applied in wastewater treatment ranging from wastewater containing colour[11], turbidity[12], chemical oxygen demand; COD[13], grease and oil[14], total suspended solids; TSS[9], heavy metals[15, 16]. Coagulation-flocculation is considered a chemical treatment because of the addition of a coagulant. Typical coagulant agents are the inorganic salt such as aluminium (III) sulphate ($Al_2(SO_4)_3$) or iron (III) chloride ($FeCl_3$), as well as synthetic organic polymer[17, 18]. Although these chemicals are rather effective in removing contaminants from aqueous solutions, several disadvantages have recently arisen, such as their impact on human diseases like Alzheimer's caused by inorganic salts and neurotoxin caused by acrylic amid[19]. Natural polymer coagulants (plant-based) are of emerging trend by many researchers because of their abundant source, low price, environmentally friendly, multifunctional, and biodegradable in water. Cowpea (*Vigna unguiculata*) is a legume of West African origin whose seeds are rich in protein and widely consumed by poor populations throughout the tropics. Cowpea seed as shown in Fig. 1, is a nutrition component in the human diet as well as livestock. It is a good source of dietary protein. Protein extracts from cowpea seed have a molecular weight of between 6–16 KDa and are cysteine-rich cationic polypeptides[20].

The potential of using active proteins agent from *Vigna unguiculata* in decolourization of AR 66 dye (Biebrich scarlet) in aqueous solution was studied. Full characterization and fiber-metric studies of the coagulant were done. The novel approach of extracting active coagulant agent

was adopted in the coagulation-flocculation process. In addition, choices of coagulant type and dye ionic nature were necessary for high-efficiency jar test performance. The response surface methodology (RSM) was used to determine the optimum operating conditions and also to determine the best area that satisfied the operating specifications.

Figure 1. Dry Cowpea (*Vigna unguiculata*) seeds

MATERIAL AND METHODS

Preparation of Coagulants

Dry seeds of the precursor were bought from local market of Enugu city, Nigeria. Matured seeds showing no signs of discolouration, softening or extreme desiccation was used. The seeds were sun dried at 35°C. The seeds were ground to fine powder (63–600 μm) using an ordinary food processor to achieve solubilization of active ingredients. The seed powder was then used in each experiment.

Extraction of Active Component

The active component from coagulant was extracted by first adding 2 g of the powdered sample in 100 ml of distilled water to make a suspension. The suspension was stirred at 120 rpm using a magnetic stirrer for 20 min at room temperature to accomplish extraction and also to enhance and activate the cationic agent present in the precursor. A local sieve cloth was used to filter the suspension to enable nano, micro, and macro-particles to be present in the filtrate for an enhanced adsorption--flocculation. The resultant filtrate solution was used as coagulants. Fresh solutions were prepared daily and kept refrigerated to prevent ageing effects (such as a change in pH, viscosity and coagulation activity). Before each experiment, solutions were shaken vigorously and used immediately for each sequence of the experiment.

Characterization of the Coagulants

Yield, bulk density, moisture content, ash content, protein content, fat content, carbohydrate content, and fibre content of the seed powder were determined by the standard official methods of analysis[21]. Fourier-Transform Infrared (FTIR) spectrometer supplied by IR Affinity-1, Shimadzu Kyoto, Japan, was used to study the chemical structure and functional groups present in the sample. The spectra were measured in the mid-infrared range (4000–400 cm^{-1}). Surface structure, morphology and fibre-metric/pore measurements of the seed powder were carried out using scanning electron microscope (SEM) supplied by Phenom Prox., world Eindhoven, Netherlands.

Buffered Solution

All assays were done in a pH-stable medium. Buffered solutions (pH 2, 4, 6, 7, 8 and 10) were prepared by the standards established according to the National Bureau of Standards (NBS) and were standardized using a digital pH meter. All reagents used were of analytical purity grade.

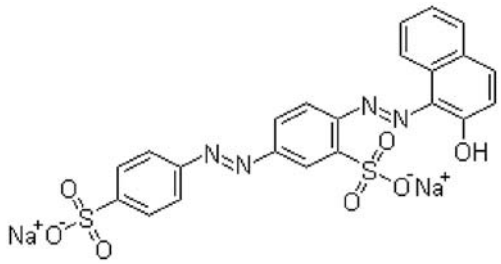

Figure 2. The structure of Biebrich scarlet dye (Acid red 66)

Table 1. Physical properties of Biebrich scarlet dye

Property	Data
Chemical Name	Sodium 6- (2-hydroxyna phthylazo) – 3, 4' – azodibenzenesulfonate.
Chemical formula	$C_{22}H_{14}N_4Na_2O_7S_2$
Molecular Weight	556.48
CAS number	4196 – 99 – 0
ECC number	224 – 084 – 5
Melting point	181 – 188°C.
UV /visible Absorbance	Max (water): 505+ 6 nm.
C.I number	26905
Class	Azo
C.I name	Acid Red 66
Common name	Biebrich scarlet.

Dye preparation and Spectrophotometric Decolourization Procedures

Acid Red 66 (AR 66), water soluble dye was provided by May & Baker England with molecular structures as shown in Fig. 2. Physical characteristics of the acid dye were summarized in Table 1. Dye with commercial purity was used without further purification. The absorption spectrum of the dye was obtained by dissolving 1000 mg/l of AR 66 in distilled water. A sample of the solution was scanned against the blank of distilled water in the range of 250–850 nm using UV-Vis spectrophotometer (Shimadzu, Model UV–1800). The maximum wavelength (λ_{max}) of 536 nm was obtained as shown in Fig. 3. A stock solution of 1000 mg/l of dye was prepared by dissolving accurately weighed amounts of AR 66 in separate doses of 1l distilled water. The desirable experimental concentrations of 10–50mg/l were prepared by diluting the stock solution when necessary. The wavelength of maximum absorbance (λ_{max}) and calibration curve at λ_{max} were determined.

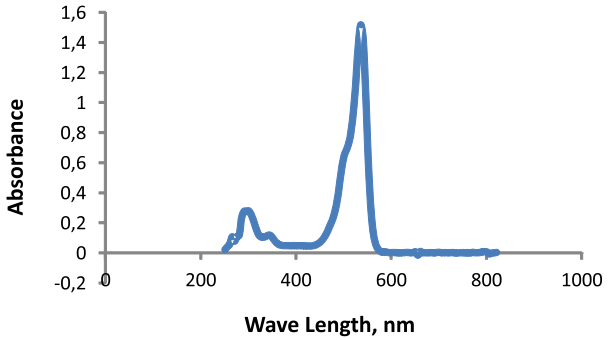

Figure 3. Spectrum peak report for AR 66

Coagulation Studies

A conventional jar test apparatus supplied by Phipps and Bird, VA, USA, equipped with six beakers of 1l capacity and six paddle stirrers was used to perform the coagulation-flocculation experiment. The jar test was conducted to evaluate the coagulation performance of the coagulants agent extracted and to establish the best operating condition for the coagulation-flocculation process. The procedure involved 4 min of rapid mixing at 100 rpm. The mixing speed was reduced to 40 rpm for another 25 min. The study was conducted by varying few experimental parameters including pH, coagulants dosages, dye concentrations and time. The pH was adjusted to the desired value using 0.1M HCl and 0.1M NaOH. All the suspensions were left for settling at a varying time between 60–540min. Supernatant samples were withdrawn after settling for absorbance analysis using UV-Vis spectrophotometer (752 W, China). Colour concentration (mg/l) measurement was determined by comparing absorbance to concentration on a calibration curve. The colour removal efficiency was obtained according to Eq. (1).

$$\text{Colour removal } (\%) = \left(\frac{C_0 - C}{C_0}\right) \text{x } 100 \quad (1)$$

where C_0 and C are the initial and final colour concentration (mg/l) in dye solutions before and after coagulation-flocculation treatment, respectively.

Experimental Design and Data Analysis

In this study, RSM was used to develop a mathematical correlation between the operating variables affecting the dye removal. Central composite design (CCD), a very efficient design tool for fitting the second-order models was used in the experimental design. The CCD was well suited for fitting quadratic surfaces, which usually works well for the process optimization[22]. Face-centred central composite design (FCCD) was implemented in the CCD. A CCD was made face-centred by the choice of $\alpha = 1$[23]. FCCD is having the position of the star points at the face of the cube portion on the design[24]. The face-centred option ensured that the axial runs will not be any more extreme than the factorial portion. The independent variables selected for this study were pH (A), coagulant dosage (B), dye concentration (C), and time (D). A 2^4 two-level factorial for four independent variables consisting of 16 factorial points coded to the usual ± notation, 8 axial points and 6 replicates at centre point were conducted, given a total of 30 experiments. Mathematically, Eq. (2) was used to determine the total number of runs performed. The total number of experiments, N is:

$$N = 2^k + 2k + n \quad (2)$$

where k is the number of factors and n is centre points.

The experimental design table is presented in Table 2. For statistical calculations, the variables Z_i (the real value of an independent variable) were coded as X_i (dimensionless value of an independent variable) according to Eq. (3):

$$X_i = \frac{Z_i - Z_i^*}{\Delta Z_i} \quad (3)$$

where Z_i stands for the uncoded value of ith independent variables, Z_i^* stands for the uncoded value of ith independent variables at the centre point and ΔZ_i is a step change value.

Design-expert software (version 9, State Ease, Minneapolis, USA) was used to analyse the experimental data fitted to a second-order polynomial model to optimize the variables in the coagulation-flocculation process. Design-expert also demonstrated the analysis of variance (ANOVA). The response was used to develop an empirical model which correlated the response to the dye coagulation-flocculation variables using a second-degree polynomial equation as given by Eq. (4):

$$Y = b_0 + \sum_{i=1}^{n} b_i X_i + \sum_{i=1}^{n} b_{ii} X_i^2 + \sum_{i=1}^{n-1} \sum_{j=i+1}^{n} b_{ij} X_i X_j + \varepsilon \quad (4)$$

where Y is the predicted response, b_0 the constant coefficient, b_i the linear coefficients, b_{ii} the quadratic coefficients, b_{ij} the interaction coefficient, X_iX_j are the coded values of the variables, n is the number of independent test variables and ε is the random error.

Adequacy of the proposed model was revealed using the diagnostic tool provided by analysis of variance (ANOVA). The quality of the model fit was expressed by the coefficient of determination (R^2). The R^2 value provides the extent of variability in the interaction between the response and the factors. The analysis was done by means of Fisher's 'F' test and P-value (probability). Model terms were evaluated by the P-value using 95% confidence level[24]. The optimum operating conditions of the colour removal were obtained by analysing the main effects plots, contour plots and overlaid contour plotting using Minitab 16 software.

Table 2. Levels and range of the variables tested in the CCD design

Variables	Factors	Units	Range and levels				
			Lowest −α	Low −1	Centre 0	High +1	Highest +α
pH (X_1)	A	–	2	2	6	10	10
Coagulants dosage (X_2)	B	mg /l	200	200	600	1000	1000
Dye concentration (X_3)	C	mg/l	10	10	30	50	50
Time (X_4)	D	min	60	60	300	540	540

RESULTS AND DISCUSSION

Characterization Result of the VUC

Proximate composition

The proximate analysis of coagulant precursor was summarized in Table 3. The moisture content values showed the water absorption ability of the coagulants. High crude protein value of 25.14% recorded in the precursor indicated the presence of protein, which is in agreement with the literature that the protein content of the precursor is cationic polypeptides (long chains of amino acids held together by peptide bonds)[20]. Fibre content present established the precursor as an organic polymer with repeating small molecules that could extend as tails and loops when dispersed in water[25]. These characteristics lead to a new discovery of an adsorption mechanism as relevant in the process. The presence of protein, moisture, carbohydrate and fibre, justified the use of the plant seed powder as a coagulant in this work.

Table 3. Proximate compositions of *Vigna unguiculata*

S/No.	Parameters	Values
1.	Yield	11.5
2	Bulk density [g/ml]	0.299
3.	Moisture Content [%]	9.0
4.	Ash content [%]	3.48
5.	Protein content [%]	25.14
6.	Fat content [%]	0.53
7.	Fibre content [%]	6.78
8.	Carbohydrate [%]	55.07

FTIR spectrometer

Figures 4 and 5 represent the FTIR peaks of VUC before and after coagulation-flocculation studies, respectively. Figure 3 showed that there is an absorption peak of 3656.92 cm^{-1} which is attributed to the stretching vibration of -OH groups and to the vibration of water absorbed, or complexes in the coagulant[26]. The free hydroxyl groups present in the spectral confirmed the presence of carboxylic acids, alcohols, and phenols on the coagulant. This band also corresponds to the –OH stretching vibrations of cellulose, pectin, and lignin[27]. The result from proximate analysis shown in Table 3 agrees with the –OH signalling of the presence of moisture (water), oil and carbohydrate. The FTIR spectral studies revealed that the characteristic absorption peak for amines was evident in 3656.92 cm^{-1} for aliphatic primary amine (N-H stretch). The presence of N-H stretching signals in the peaks detects the presence of amino compounds which confirms protein contents present in the coagulant as evident in Table 3. A major band present in the coagulants in the broad region of 2083.06–1867.04 cm^{-1} usually indicates the presence of a C=O group (carbonyl compound). The FTIR peaks show that some peaks were shifted or disappeared as can be seen in 3286.60 cm^{-1} and 2700.26 cm^{-1} and the new peaks were also detected. These changes as observed in the functional groups -C=C-H, C=CH, C-H

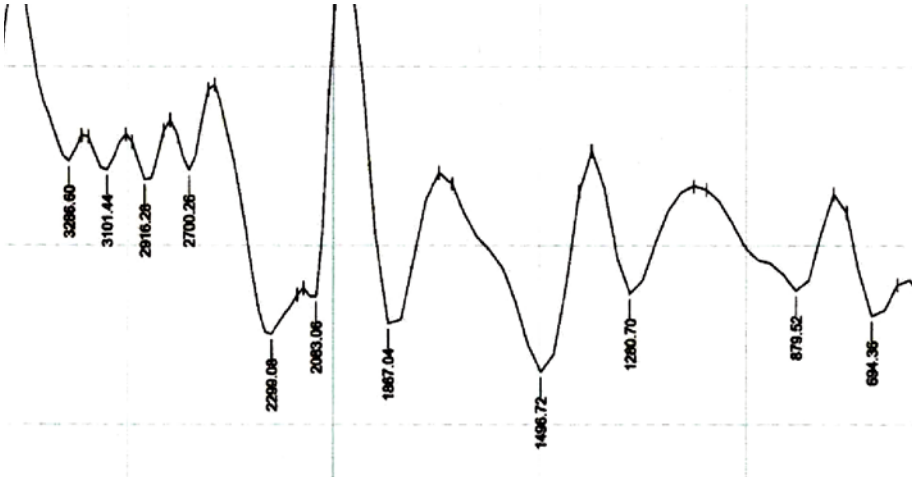

Figure 4. FTIR transmittance spectrum of VUC before Coagulation-flocculation studies

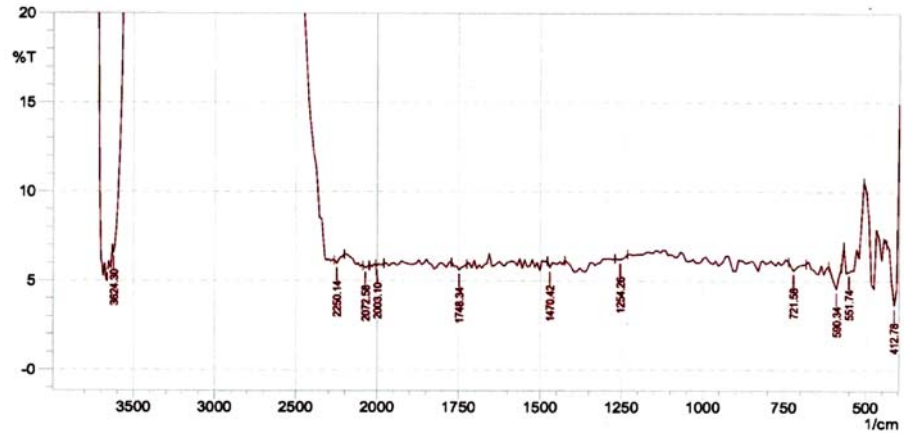

Figure 5. FTIR transmittance spectrum of VUC after Coagulation-flocculation studies

stretching and $–CH_2–$, was an indication of the possible involvement of those functional groups on the coagulation-flocculation and surface adsorption of the particles on to polymer surfaces. The diminished peaks showed that all the functional groups are completely involved in the process. The FTIR spectral of *Vigna unguiculata* and the proximate analysis suggested the presence of moisture, proteins, and esters, which justified its presence involvement as a coagulant.

SEM Result

The surface morphologies of VU in 600x and 1000x magnifications before and after coagulation studies are shown in Fig. 6. Figure 6a revealed pores of different shapes and sizes. The pore sizes (micro-pores, macro-pores, and meso-pores) are properties that are unique to organic polymers. Rough surface as observed shows that the coagulant is coarse fibrous substance largely composed of cellulose and lignin which confirms its polymeric characteristics. Particles could be attached to these polymer chains through adsorption, inter-particle bridging or electrostatic contacts. The morphology also possessed a compact-net structure which is more favourable to particle coagulation-flocculation due to adsorption and bridge formation among flocs as compared to branched structure[28]. Figure 6b showed large clusters due to flocculation of particles. There is also an adsorption of particles on polymer surface given that the number of pores on the polymer surfaces was reduced or filled up[29].

In combination with the Phenom™ desktop, scanning electron microscope, the fiber-metric application allows you to produce accurate size information from micro and nano fibre samples. SEM is also a novel technique used on bio-aggregates in order to improve our understanding of their porosity, pore size distribution, pore connectivity, and micro structure, all of which are characteristics that are essential to the benefits of using biomass. The pore size measurement result is presented in the histogram as shown in Fig. 7. In the histogram, there is a hierarchy of pore types that range from micro-pore to meso-pore to fracture macropores. The minimum/maximum and average fibre size are also displayed below the histogram. Figure 8 shows the predefined pore measurement areas for fiber-metric image and pore distribution. It revealed

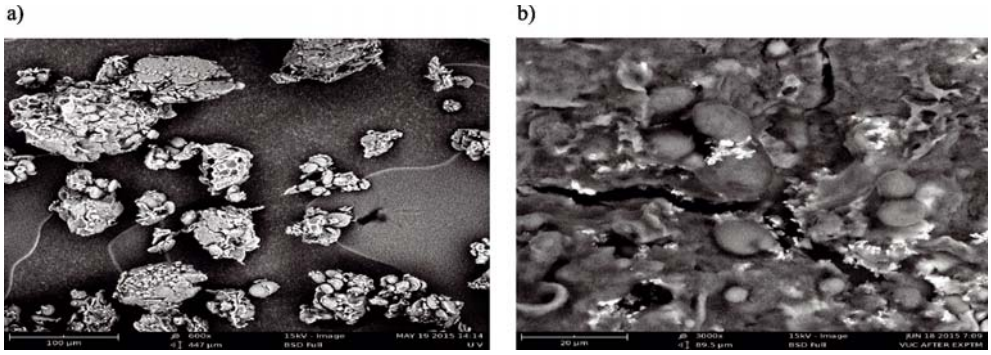

Figure 6. SEM Micrograph of VUC before (a) and after (b) coagulation experiment

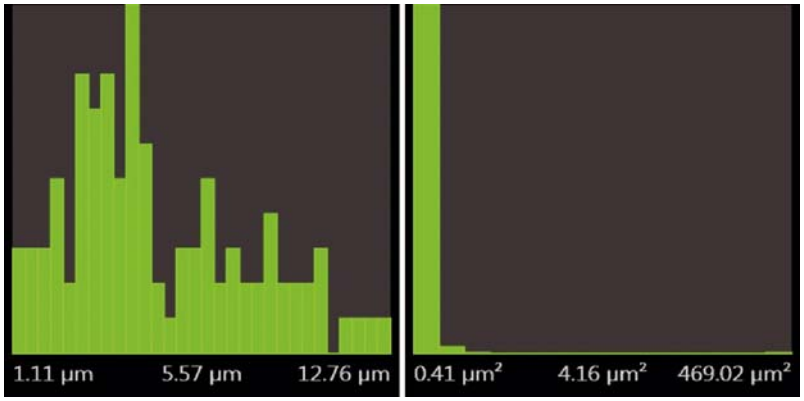

Figure 7. Pore size histogram measurement

Figure 8. Fibre metric image measurement and pore distribution

an automated pore measurement on a polymer membrane sample.

Development of Regression Model

To study the factor interactions, experiments were performed for different combinations of the factors. The responses to the combinations were obtained. The experimental design matrix showing the coded and uncoded factor combinations together with the experimental (exp) and predicted (pre) decolourization efficiencies are shown in Table 4.

The adequacy of the model was justified through ANOVA as shown in Table 5. The quadratic regression analysis shows the model was significant at 95% confidence level by the Fisher's testing. This was confirmed having obtained the F-value of 90.74. The P-value result of less than 0.05 (P-values of regression ≤ 0.05) showed statistically significant model. The models did not exhibit lack-of-fit indicating insignificant lack-of-fit.

The coefficient of determination (R^2) measures the model's overall performance. Greater than 0.2 differences between predicted R^2 and adjusted R^2 indicate that non-significant term may be included in the model[23]. A high R^2 value, close to 1, is desirable and ensures a satisfactory adjustment of the quadratic model to the experimental data. The R^2 value of 98.83% indicated the model total variation is 1.17% which is in an acceptable range. The difference between the value of predicted R^2 and adjusted R^2 was 0.029 that is less than 0.2 indicating the accuracy of the model. It was observed from Table 5 also that the coefficient terms (A, B, C, and D) and square terms (A^2 and B^2) were significant to the

Table 4. CCD in coded and uncoded form and response result for colour removal from AR 66

Std Order	Run Order	A: pH [X_1]		B: VUC Dosage [X_2, mg/l]		C:Concentration [X_3, mg/ l]		D: Time [X_4, min]		Y_{vuc} Colour removal [%]	
		Coded	Uncoded	Coded	Uncoded	Coded	Uncoded	Coded	Uncoded	Experimental [exp]	Predicted [pre]
17	1	–1	2	0	600	0	30	0	300	75.6	81.01
28	2	0	6	0	600	0	30	0	300	36.5	37.81
20	3	0	6	1	1000	0	30	0	300	31	28.12
9	4	–1	2	–1	200	–1	10	1	540	98.2	99.26
8	5	1	10	1	1000	1	50	–1	60	19.5	19.35
16	6	1	10	1	1000	1	50	1	540	49.8	51.97
2	7	1	10	–1	200	–1	10	–1	60	36.8	38.47
7	8	–1	2	1	1000	1	50	–1	60	50	50.15
22	9	0	6	0	600	1	50	0	300	32.9	31.65
1	10	–1	2	–1	200	–1	10	–1	60	75.4	72.97
24	11	0	6	0	600	0	30	1	540	57.2	53.42
5	12	–1	2	–1	200	1	50	–1	60	64.5	63.58
12	13	1	10	1	1000	–1	10	1	540	57.9	59.74
4	14	1	10	1	1000	–1	10	–1	60	27.4	28.34
27	15	0	6	0	600	0	30	0	300	36.5	37.81
25	16	0	6	0	600	0	30	0	300	36.5	37.81
26	17	0	6	0	600	0	30	0	300	36.5	37.81
19	18	0	6	–1	200	0	30	0	300	38.6	38.86
18	19	1	10	0	600	0	30	0	300	57.9	49.87
14	20	1	10	–1	200	1	50	1	540	59	60.65
3	21	–1	2	1	1000	–1	10	–1	60	60.9	60.16
11	22	–1	2	1	1000	–1	10	1	540	89.1	88.53
10	23	1	10	–1	200	–1	10	1	540	68.2	67.79
15	24	–1	2	1	1000	1	50	1	540	80.5	79.74
13	25	–1	2	–1	200	1	50	1	540	92.3	91.10
30	26	0	6	0	600	0	30	0	300	36.5	37.81
29	27	0	6	0	600	0	30	0	300	36.5	37.81
23	28	0	6	0	600	0	30	–1	60	22.8	23.96
21	29	0	6	0	600	–1	10	0	300	41.6	40.23
6	30	1	10	–1	200	1	50	–1	60	29.8	30.11

Table 5. ANOVA response result

Y_{vuc}	Source	Sum of Squares	df	Mean Square	F Value	p-value Prob> F		R- Squared
	Model	13300.66	14	950.05	90.74	< 0.0001	significant	
	A-pH	4361.78	1	4361.78	416.59	< 0.0001		
	B-Dosage	519.49	1	519.49	49.62	< 0.0001		
	C-Dye Concentration	331.10	1	331.10	31.62	< 0.0001		
	D-Time	3904.33	1	3904.33	372.90	< 0.0001		
	AB	7.16	1	7.16	0.68	0.4214		
	AC	1.05	1	1.05	0.10	0.7558		
	AD	9.15	1	9.15	0.87	0.3647		
	BC	0.39	1	0.39	0.037	0.8494		
	BD	4.31	1	4.31	0.41	0.5310		
	CD	1.50	1	1.50	0.14	0.7103		
	A^2	1977.54	1	1977.54	188.87	< 0.0001		
	B^2	48.42	1	48.42	4.62	0.0382		
	C^2	9.09	1	9.09	0.87	0.3663		
	D^2	1.99	1	1.99	0.19	0.6688		
	Residual	157.05	15	10.47				
	Lack of Fit	157.05	10	15.71				
	Pure Error	0.000	5	0.000				
	Cor Total	13457.71	29					
	R - Squared							0.9883
	Adjusted R - Squared							0.9774
	Pred R - Squared							0.9488

response whereas the interaction terms (AB, AC, AD, BC, BD, and CD) were insignificant to the response.

Second-order quadratic Eqs 5 and 6 show the final empirical equations in terms of coded and actual factors, respectively after excluding the insignificant terms. Positive signs in front of the equations indicate an interactive positive effect among the factors. In conclusion, the quadratic model for the response measured is significant and adequate.

$$Y_{vuc} = +37.8114 + -15.5667 * A + -5.37222 * B + -4.28889 * C + 14.7278 * D + 27.6272 * A^2 + -4.32281 * B^2 \quad (5)$$

$$Y_{vuc} = +111.52955 - 25.19526 * pH + 0.015448 * Dosage + 0.039836 * Dye\ concentration + 0.042346 * Time + 1.72670 * pH^2 - 2.70175E\text{-}005 * Dosage^2 \quad (6)$$

A reliable model should have a good prediction with experimental data. There is a good agreement between the actual removal efficiency (%) and predicted removal efficiency (%) as shown in Fig. 9. The observed points reveal that the actual values are distributed relatively near the straight line in most cases, showing a good prediction by the model. A close relationship between predicted and actual data indicates a good fit.

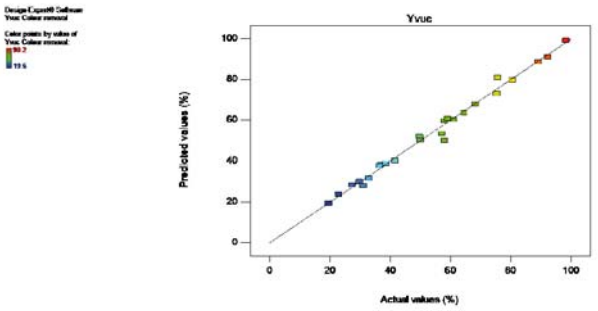

Figure 9. Equality plot for the actual and predicted values of Y_{vuc} colour removal (%)

Evaluation of Operation Parameters

Main effects plot (data means) for Y_{vuc} colour removal (%)

The main effect plot for the factors affecting the colour removal is shown in Fig. 10. The solution pH has the highest effect on the process. There were higher colour removals at low pH values as observed in Fig. 10a. Its impact on the colour removal efficiency was highest at 2 having the efficiency of 76.3%. This trend will be explained further by the charge on the hydrolysis products and precipitation of polymeric hydroxides which are both controlled by pH variations[30]. As the functional groups of the acid dyes are anionic, hydrolysis products of the organic biopolymer can neutralize the negative charges on dye molecules followed by flocculation which is enhanced by polymer adsorption, sweep-flocculation or inter-particle bridging. Charge neutralization, sweep-flocculation, polymer adsorption and inter-particle bridging could have played a predominant role in the coagulation-flocculation process due to the optimum pH value. Generally, adsorption of the organic contaminants (OC) onto polymer hydroxide precipitate forming at high pH also limited. As pH increases, OC becomes more negatively charged and polymer hydrolysis species become less positively charged, resulting in lower flocculation

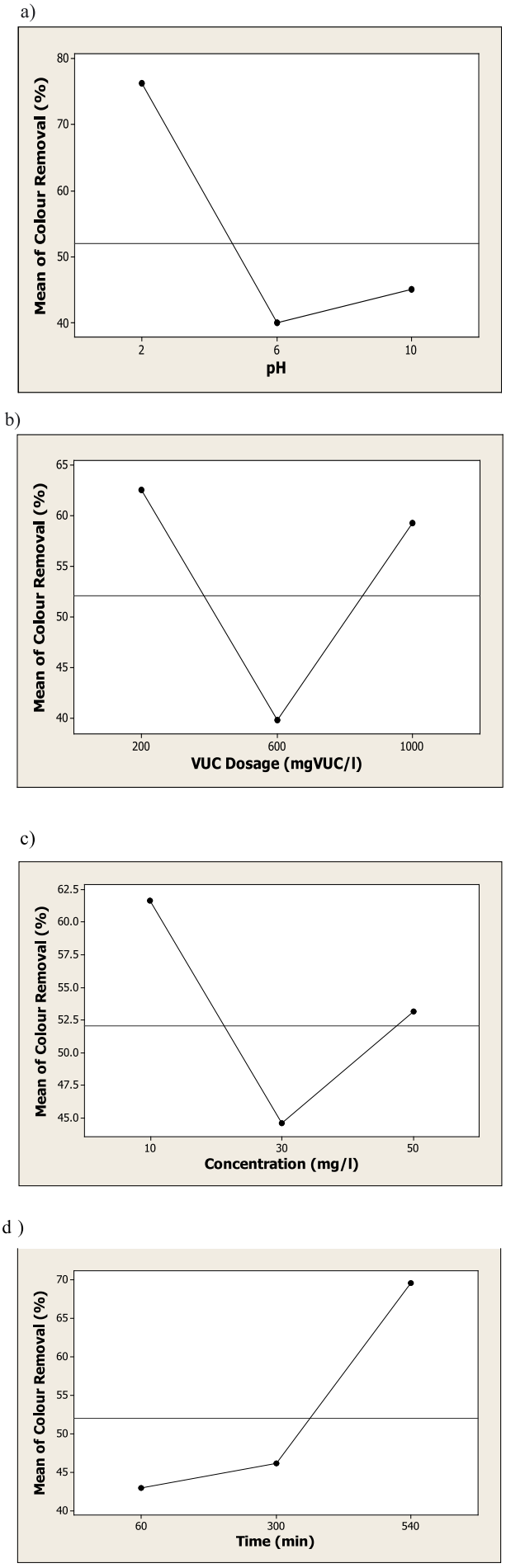

Figure 10. Main effects plot for Y_{vuc} colour removal (%): a) pH; b) VUC Dosage; c) Dye Concentration; and d) Settling Time

tendency. Therefore, coagulation-flocculation of OC in wastewater is recommended to be performed under low pH conditions along with the presence of soluble cationic polymer hydrolysis species. These species react with anionic functional groups on OC to precipitate as a polymer-OC. In conclusion, high removal efficiency at low pH values is predominant in OC removal from acid dyes. Similar results were reported by Beltran and Sanchez[31] and Moghaddan[20].

The plot as shown in Fig 10b indicates the effect of VUC dosage on colour removal. Highest colour removal was achieved at 200mgVUC/l with the efficiency of 62.5%. Charge-neutralization and adsorption mechanism was observed to be predominant mechanism in the colour removal due to high efficiency at low dosage. The use of cationic polymer for coagulation-flocculation of negatively-charged colour particles is needed because strong adsorption affinity and neutralization of the particle charges could occur during the process. The high dosages of the organic polymer could give rise to chain bridging and adsorption mechanism[32] which resulted in high removal as observed in Fig. 10b.

The concentration of dye provides an important driving force to overcome all the mass transfer resistance of the dye between the aqueous and solid phases. The effect of dye concentration on the colour removal efficiency is shown in Fig. 10c. The plot indicates that dye concentration has the lowest effect on the colour removal efficiency. Its effect on the removal efficiency was highest at 10mg/l with the efficiency of 61.7%.

Flocs formation involves both interactions of coagulant hydroxide precipitate following the hydrolysis reaction and contact with particles[33]. Coagulation-flocculation performance is mostly evaluated through a time-dependent decrease in particle concentration and consequently, coincides with the growth of aggregates. Figure 10d shows that the highest reduction in concentration was at 540min resulting in removal efficiency of 70%. The plot indicates that time has a significant effect on the removal process. Longer flocculation time (60–540 min) in this process confirmed further the presence of adsorption mechanism.

Response surface and contour factor interactions.

The 3D surface plots and its corresponding contour plots are represented in Fig. 11 for better interacting factor effects for efficient decolourization of the process. The plots show that the maximum removal efficiency was in the range of pH 2–4, coagulant dosage from 200–300 mg/l, dye concentration from 10–20 mg/l and time from 350–540min. The response surface plots gave an indication that the maximum colour removal efficiencies are located inside the design boundary.

The pH must be controlled in order to establish optimum conditions in the process. The effectiveness of the coagulant is highly dependent on pH as shown in Fig. 11. The polymers showed higher colour removals at low pH values. The result also indicated that removal efficiencies increased more at lower coagulant dosages. Maximum colour removal efficiency was achieved at coagulant dosages between 200–400 mg/l. The high removal efficiencies of >82% found in the 200 mg/l dosages confirmed charge-neutralization and adsorption mechanism to be predominant mechanisms in the studied dosage range. Positive charge species were responsible for removal of particles by charge neutralization. The use of cationic polymer for coagulation-flocculation of negatively-charged colour particles was appropriate because strong adsorption affinity and neutralization of the particle charges could occur. High percentage removals observed at high dosages of the organic polymer were as a result of sweep flocculation and adsorption mechanisms, which are inclined to occur at high dosages[13].

Figure 11 finally showed that the reduction in colour concentration did not vary significantly after 540 min showing equilibrium was achieved after 540 min. Destabilization of the aggregate flocs could set in after this time due to saturation of the active sites.

Optimization Analysis

Minitab 16 was used to optimize the colour removal efficiency. Process optimization searches for a combination of factor levels that simultaneously satisfy the criteria placed on each response and factors. Numerical optimization was employed and the desired maximum goal was set for each factor and responses. These goals were combined into an overall desirability function, for effective maximization of the function. Optimal conditions and the optimization results are shown in Table 6.

Model validation and confirmation experiments.

The optimum predicted values were further validated by carrying out the experiment at the optimal predicted conditions and the results of the experimental values were also shown in Table 6. The experimental data confirm good agreements with RSM results. The verification experiments demonstrated a good agreement between the experimental and predicted, indicating RSM approach adopted was appropriate for optimizing the coagulation--flocculation process. The standard error (%) between the predicted and the experimental value of 1.96% was obtained. The value was less than 4% indicating very good prediction by the model. The adequacy of the model was once again verified effectively by the experimental data validation

Table 6. Confirmation result of the model using optimum predicted values

Variables	Units	Optimum Values
pH	–	2
VUC Dosage	mg/l	256.09
Dye Concentration	mg/l	16.7
Time	min	540
Colour removal efficiency (predicted)	%	99.26
Colour removal efficiency (experimental)	%	97.31
Standard Error	%	1.96

Overlaid contour plots

The overlaid contour plot (OCP) is used to visually identify an area where the predicted means of the response variable is in an acceptable range. A compromise among the optimum conditions for response is desirable. The desirability function approaches together with graphical optimization was used to achieve this goal[24]. By defining the desired limits, the optimum condition can be visualized graphically by superimposing the factors

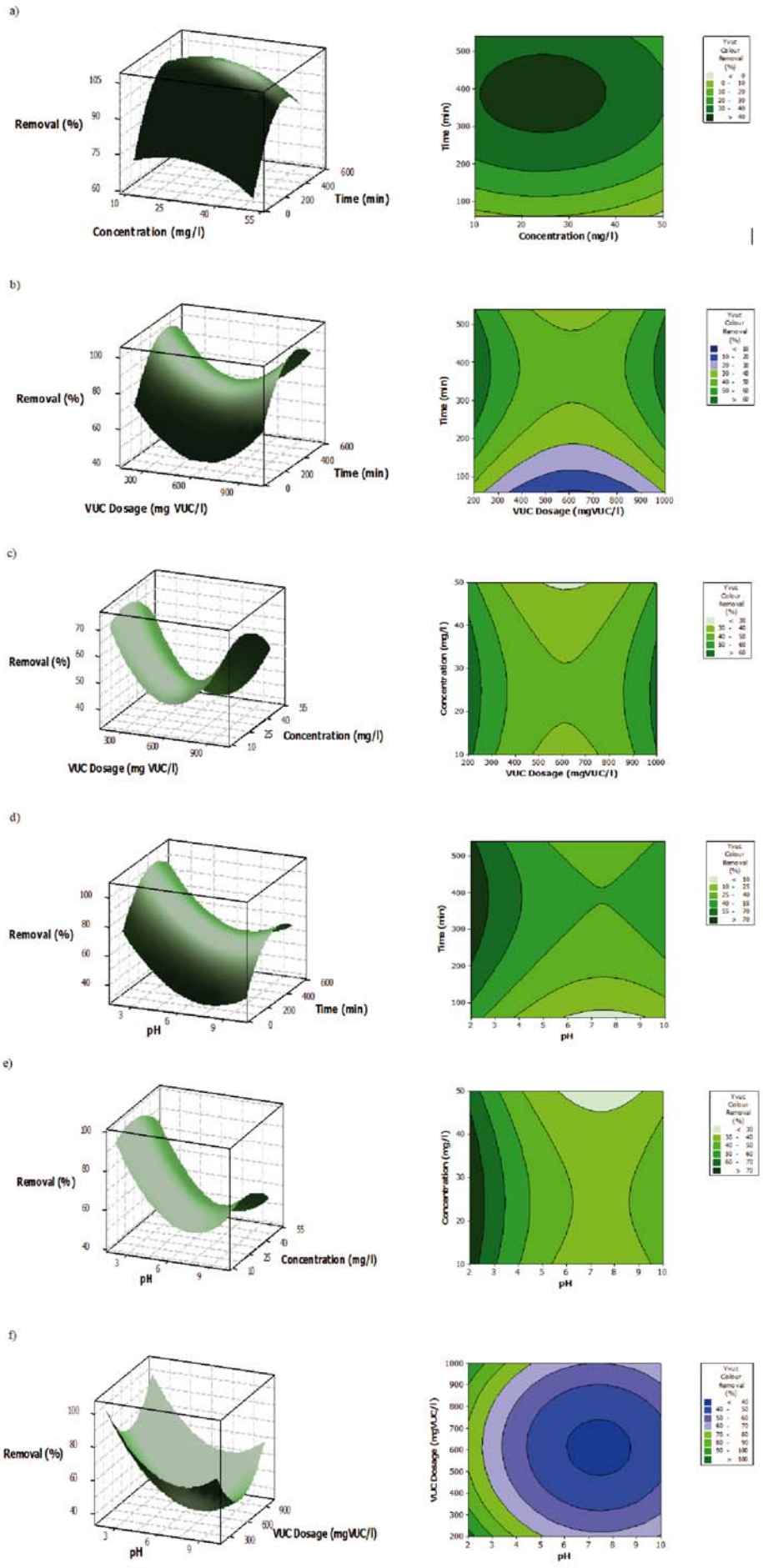

Figure 11. 3D Surface and its corresponding contour plots for colour removal as a function of a) dye concentration and time at pH of 2 and dosage of 200 mg/l; b) dosage and time at pH of 2 and dye concentration 10 mg/l; c) dosage and dye concentration at pH of 2 and time of 300 min; d) pH and time at dosage of 200 mg/l and dye concentration of 10 mg/l; e) pH and dye concentration at dosage of 200 mg/l and time of 300 min; f) pH and dosage at dye concentration of 10 mg/l and time of 300 min

in an OCP, as shown in Fig. 12. The white shades are the optimum predicted regions showing the areas that satisfy the response goal of greater than or equal to 80% colour removal for the factor interactions at mid hold values. Areas that do not fit the optimization criteria were shaded gray. OCP is mostly applied when there is an emergency because it reduces preparation time and experimental cost. It shows clearly the high efficient region of the contour.

particles, to enhance flocs formation due to its polymer characteristics and to adsorb particles on its surfaces due to its different pores and rough surfaces. The experimental results were statistically analysed with RSM technique by implementing FCCD. From the study, pH and time were the most influencing factors in the colour removal process. The optimal conditions from the main effects (data means) plot were pH 2, coagulant dosage 200 mg/l, dye concentration 10mg/l and time 540min

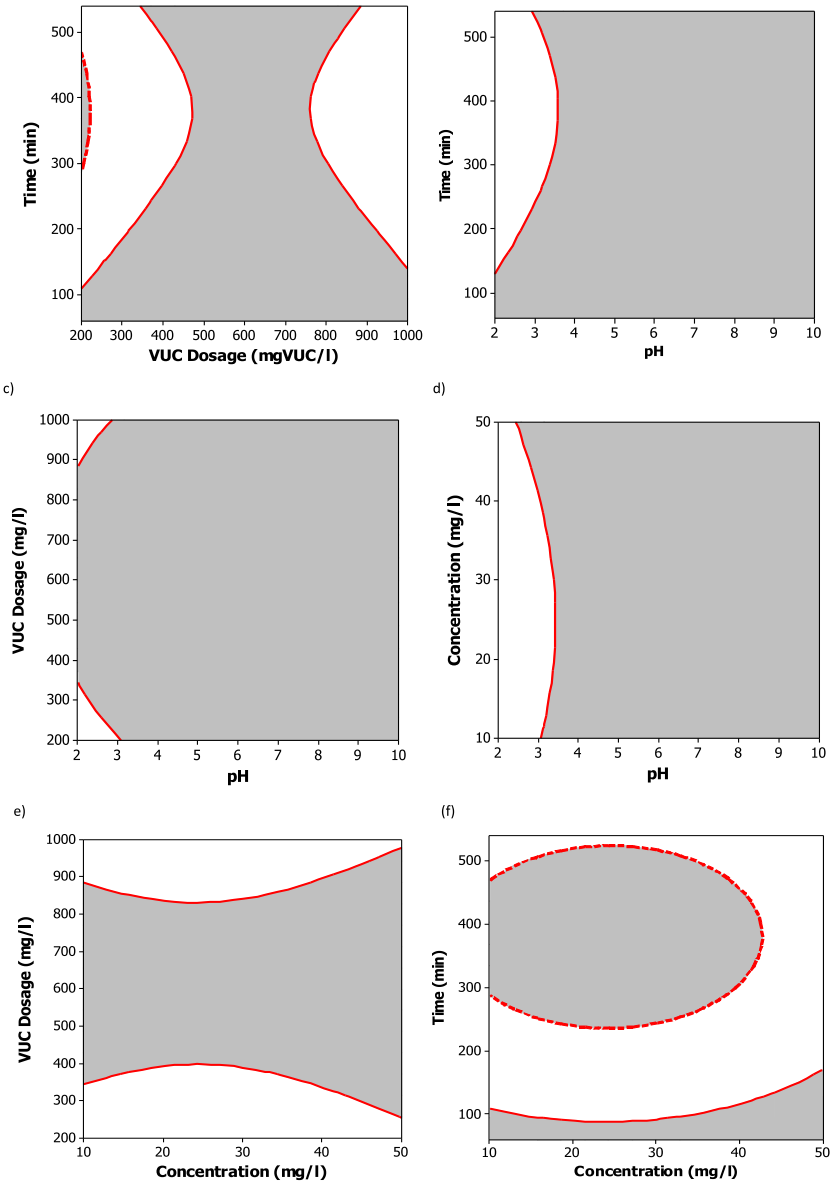

Figure 12. Overlaid Contour Plots for Colour Removal (%): (a) time and dosage at pH of 2 and dye concentration 10 mg/l; (b) time and pH at dosage of 200 mg/l and dye concentration of 10 mg/l; (c) dosage and pH at dye concentration of 10 mg/l and time of 540 min; (d) dye concentration and pH at dosage of 200 mg/l and time of 540 min; (e) dosage and dye concentration at pH of 2 and time of 540 min; (f) time and dye concentration at pH of 2 and dosage of 200 mg/l

CONCLUSION

Coagulation behaviour of *Vigna unguiculata* (VU) was tested on the effect of four operating parameters, namely; pH, coagulant dosage, dye concentration and time. Proximate analysis result showed that VUC has the characteristics of a potential coagulant. FTIR analysis indicated that some chemical bonds such as -OH, N-H, C=H were present in the coagulant precursor. SEM image revealed rough surfaces, different pores sizes, and compact-net structure. The characterization result showed the coagulant ability; to destabilize contaminant coagulation-flocculation. Pore measurement and rough surfaces observed on the coagulant morphology confirmed that adsorption was an important mechanism in the coagulation-flocculation process. The colour removal efficiency obtained from the optimization analysis was 99.26% at process conditions of pH 2, coagulant dosage 256.09mg/l, dye concentration 16.7mg/l and time 540min. Further confirmation experiments demonstrated a good agreement with the predicted values, indicating that FCCD was an effective optimization tool for the coagulation-flocculation process. There was a higher removal

efficiency using the FCCD model as compared to the efficiency obtained from the main effect plot.

LITERATURE CITED

1. Vinicius, C., Flavio, B.F. & Karina, Q.D. (2013). Treatment of textile effluent containing indigo blue dye by a UASB reactor coupled with pottery clay adsorption. *Acta Scientiarum Technology*. 35, 53–58. DOI: 10.4025/actascitechnol.v35i1.13091.

2. Zonoozi, M.H., Moghaddam, R.M., Arami, A.G. (2008). Removal of Acid Red 398 dye from aqueous solutions by coagulation/flocculation process. *Environ. Eng. and Manage. J*. 7, 695–699.

3. Roop, G. & Meenakshi, G. (2005). Activated carbon Adsorption; Adsorptive removal of organics from water. *Taylor and Francis Group*. Pg 373–375.

4. Liu, Y., Wang, J., Zheng, Y. & Wang, A. (2012). Adsorption of methylene blue by Kapok fibre treated by sodium chlorite optimized with response surface methodology. *Chem. Eng. J.* 184, 248–255. DOI: 10.1016/j.cej.2012.01.049.

5. Shore, J. (2002). Colorants and auxiliaries organic chemistry and application properties. 2nd Ed. Bradford.

6. Shi, B.Y., Li, G.H., Wang, D.S., Feng, C.H. & Tang, H.X. (2007). Removal of direct dyes by coagulation: the performance of preformed polymeric aluminium species. *J. Hazard. Mater.* 143, 567–574. DOI: 10.1016/j.jhazmat.2006.09.076.

7. Edward, G. (1971). Synthetic dyes in biology, medicine, and chemistry. Academic press, London, England. DOI: 10.1086/407095.

8. Yee, K.O., Fu, Y.L., Shi-Peng, S., Bai-Wang, Z., Can-Zeng, L. & Tai-Shung, C. (2014). Nanofiltration hollow fiber membrane for textile wastewater treatment: from lab-scale to pilot-scale studies. *Chem. Eng. Sci.* 114, 51–57. DOI: 10.1016/j.ces.2014.04.007.

9. Qian-Cheng, X., Jue, W., Xiao, W., Bo-Zhi, C., Jia-Lin, G., Tian-Zhi, J., Shi-Peng, S. (2017). A hydrophilicity gradient control mechanism for fabricating delamination-free dual-layer membranes. *J. Membr. Sci.* 539, 392–402. DOI: 10.1016/j.memsci.2017.06.021.

10. Gosavi, V.D. & Sharma, S. (2014). A general review of various treatment methods for textile wastewater. *J. Environ. Sci. Comput. Sci. Eng. Technol*. 3, 29–39.

11. Khouni, I., Marrot, B., Moulin, P. & Amar, R.B. (2011). Decolourization of the reconstituted textile effluent by different process treatments: Enzymatic catalysis, coagulation/flocculation and nanofiltration processes. *Desalination* 268, 27–37. DOI: 10.1016/j.desal.2010.09.046.

12. Tzoupanos, N.D., Zouboulis, A.I. & Zhao, Y.C. (2008). The application of novel coagulant reagent (poly aluminium silicate chloride) for the post-treatment of landfill leachates. *Chemosphere* 73, 729–736. DOI: 10.1016/j.chemosphere.2008.06.051.

13. Zhu, G., Zheng, H., Chen, W., Fan, W., Zhang, P. & Tshukudu, T. (2012). Preparation of a composite coagulant: Polymeric aluminium ferric sulphate (PAFS) for wastewater treatment. *Desalination* 285, 315–323. DOI: 10.1016/j.desal.2011.10.019.

14. Gao, B.Y., Yue, Q.Y. & Wang, Y. (2007). Coagulation performance of poly aluminium silicate chloride (PASiC) for wastewater treatment. *Sep. Purific. Technol.* 56, 225–230. DOI: 10.1016/j.seppur.2007.02.003.

15. Cheng, R., Liang, S., Wang, H. & Beuhler, M. (1994). Enhanced Coagulation for Arsenic Removal. *American Water Works Association* 86, 79–90. DOI: 10.1002/j.1551-8833.1994.tb06248.x.

16. Beltrán-Heredia, J., Sánchez-Martín, J. (2008). Heavy metals removal from surface water with *Moringa oleifera* seed extract as flocculant agent. *Fresenius Environmental Bulletin* 17 (12), 2134–2140.

17. Obiora-Okafo, I.A., Menkiti, M.C. & Onukwuli, O.D. (2014). Utilization of response surface methodology and factor design in micro organic particles removal from brewery wastewater by coagulation/flocculation technique. *Inter. J. of Appl. Sci. and Maths*. 1(1), 15–21.

18. Papic, S., Koprivanac, N., Bozic, A.L. & Metes, A. (2004). Removal of some reactive dyes from synthetic wastewater by combined Al (111) coagulation/carbon adsorption process. *Dyes pigments* 62(2), 29–298. DOI: 10.1016/S0143-7208(03)00148-7.

19. Flaten, P. (2001). Aluminum as a risk factor for Alzheimer's disease with an emphasis on drinking water. *Brain Res. Bull*. 55 (2), 187–196. DOI: 10.1016/S0361-9230(01)00459-2.

20. Mariângela, S.S.D., André, O.C. & Valdirene, M.G. (2003). Purification and molecular mass determination of a lipid transfer protein exuded from Vigna unguiculata seeds. Braz. J. Plant Physiol. 15, 417–421. DOI: 10.1590/S1677-04202003000300007.

21. A.O.A.C. (1990). Official Methods of Analysis. 15th Edition. Association of Official Analytical Chemists. Washington DC, U.S.A.

22. Moghaddam, S.S., Alavi Moghaddam, M.R. & Arami, M. (2010). Coagulation/flocculation process for dye removal using sludge from water treatment plant: optimization through response surface methodology. Journal of *Hazard. Materials* 175, 651–657. DOI: 10.1016/j.jhazmat.2009.10.058.

23. Montgomery, D.C. (2001). Design and Analysis of Experiments. 5th Ed., John Wiley and Sons, New York.

24. Montgomery, D.C. & Myers, R.H. (2002). Response surface methodology: process and product optimization using designed experiments. 2nd Ed. John Wiley and Sons, New York.

25. Bolto, B. & Gregory, J. (2007). Organic polyelectrolyte in water treatment. *Water Res*. 41, 2301–2324. DOI:10.1016/j.watres.2007.03.012.

26. Stuart, B.H. (2004). Infrared spectroscopy: Fundamentals and Applications. John Wiley and Sons. Ltd. Pg. 45–47. DOI: 10.1002/0470011149.

27. Coates, J. (2000). Interpretation of Infrared Spectra, a Practical Approach in Encyclopedia of Analytical Chemistry. John Wiley & Sons Ltd, Chichester. Pg. 10815–10837. DOI: 10.1002/9780470027318.a5606.

28. Zheng, Y. & Park, J. (2009). Characterization and coagulation performance of a novel inorganic polymer coagulant: Poly-zinc-silicate-sulphate. Colloids and Surfaces A: Physicochem. *Eng. Aspects.* 334, 147–154. DOI: 10.1016/j.colsurfa.2008.10.009.

29. Bilal, M., Haroon, H., Gardazi, S.M.H., Butt, T.A., Pervez, A. & Mahmood, Q. (2017). Novel lingo cellulosic wastes for comparative adsorption of Cr(VI): equilibrium kinetics and thermodynamic studies. *P. J. Chem. Technol.* 19 (2), 6–15. DOI: 10.1515/pjct-2017-0021.

30. Li, G. & Gregory, J. (1991). Flocculation and sedimentation of high turbidity waters. *Water Res*. 25, 1137–1143. DOI: 10.1016/0043-1354(91)90207-7.

31. Beltran-Heredia, J., Sanchez-Martin, J., Davila-Acedo, M.A. (2011). Optimization of the synthesis of a new coagulant from a tannin extract. *J. Hazard. Mater.* 186, 1704–1712. DOI: 10.1016/j.jhazmat.2010.12.075.

32. Zhu, G., Zheng, H., Zhang, Z., Tshukudua, T., Zhang, P. & Xiang, X. (2011). Characterization and coagulation-flocculation behaviour of polymeric aluminium ferric sulphate (PAFS). *Chem. Eng. J*. 178, 50–59. DOI: 10.1016/j.cej.2011.10.008.

33. Obiora-Okafo, I.A. & Onukwuli, O.D. (2015). Optimization of a coagulation-flocculation process for colour removal from synthetic dye wastewater using natural organic polymers: Response surface methodology applied. *Inter. J. of Scientific & Eng. Research* 6 (12), 693–704.